

Обзор ArXiv:astro-ph,  
4-8 февраля 2019 года

От Сильченко О.К.

# ArXiv: 1902.01408

## Metallicity calibrations for diffuse ionised gas and low ionisation emission regions

Nimisha Kumari,<sup>1,2,3\*</sup> Roberto Maiolino,<sup>1,2</sup> Francesco Belfiore<sup>4</sup> and Mirko Curti<sup>1,2</sup>

<sup>1</sup>*Kavli Institute for Cosmology, University of Cambridge CB3 0HA, UK*

<sup>2</sup>*Cavendish Laboratory, University of Cambridge CB3 0HE, UK*

<sup>3</sup>*Institute of Astronomy, University of Cambridge CB3 0HA, UK*

<sup>4</sup>*European Southern Observatory, Karl-Schwarzschild-Str. 2, D-85748 Garching, Germany*

Accepted XXX. Received YYY; in original form ZZZ

### ABSTRACT

Using integral field spectroscopic data of 24 nearby spiral galaxies obtained with the Multi-Unit Spectroscopic Explorer (MUSE), we derive empirical calibrations to determine the metallicity of the diffuse ionized gas (DIG) and/or of the low-ionisation emission region (LI(N)ER) in passive regions of galaxies. To do so, we identify a large number of H II–DIG/LIER pairs that are close enough to be chemically homogeneous and we measure the metallicity difference of each DIG/LIER region relative to its H II region companion when applying the same strong line calibrations. The O3N2 diagnostic ( $=\log \left( \frac{[\text{O III}]/\text{H}\beta}{[\text{N II}]/\text{H}\alpha} \right)$ ) shows a minimal offset (0.01–0.04 dex) between DIG/LIER and H II regions and little dispersion of the metallicity differences (0.05 dex), suggesting that the O3N2 metallicity calibration for H II regions can be applied to DIG/LIER regions and that, when used on poorly resolved galaxies, this diagnostic provides reliable results by suffering little from DIG contamination. We also derive second-order corrections which further reduce the scatter (0.03–0.04 dex) in the differential metallicity of H II–DIG/LIER pairs. Similarly, we explore other metallicity diagnostics such as O3S2 ( $=\log \left( \frac{[\text{O III}]/\text{H}\beta}{[\text{S II}]/\text{H}\alpha} \right)$ ) and N3S2 ( $=\log \left( \frac{[\text{N III}]/\text{H}\beta}{[\text{S II}]/\text{H}\alpha} \right)$ ).

# Разделение SF-nonSF; создание «пар»

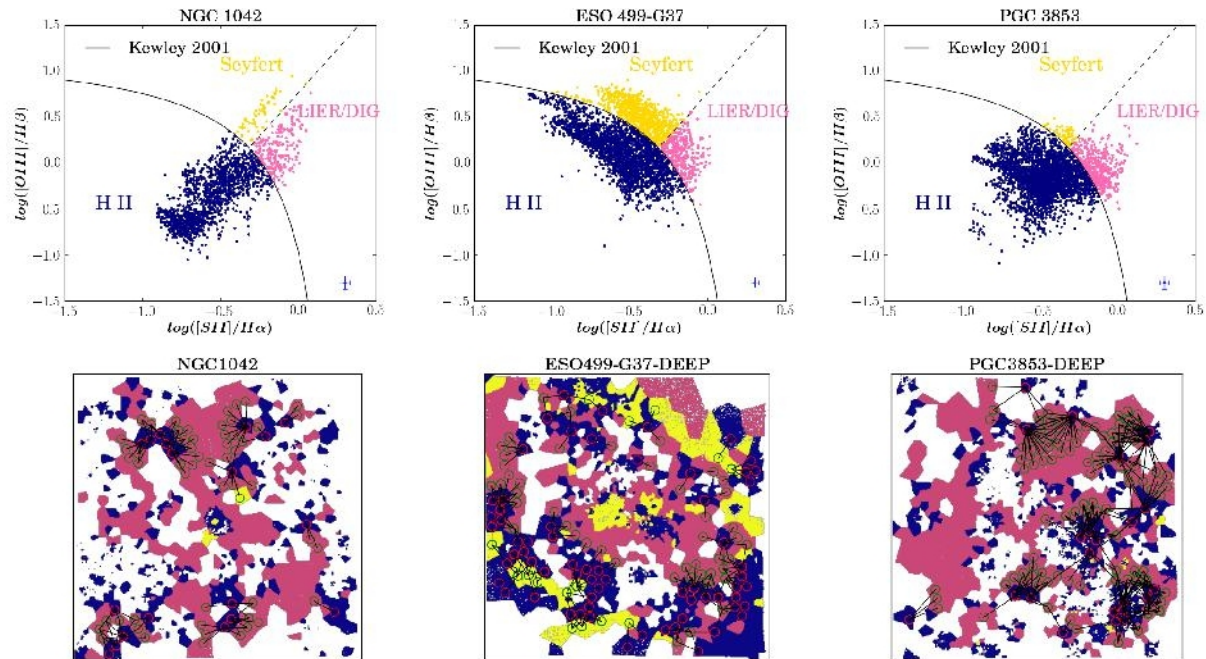
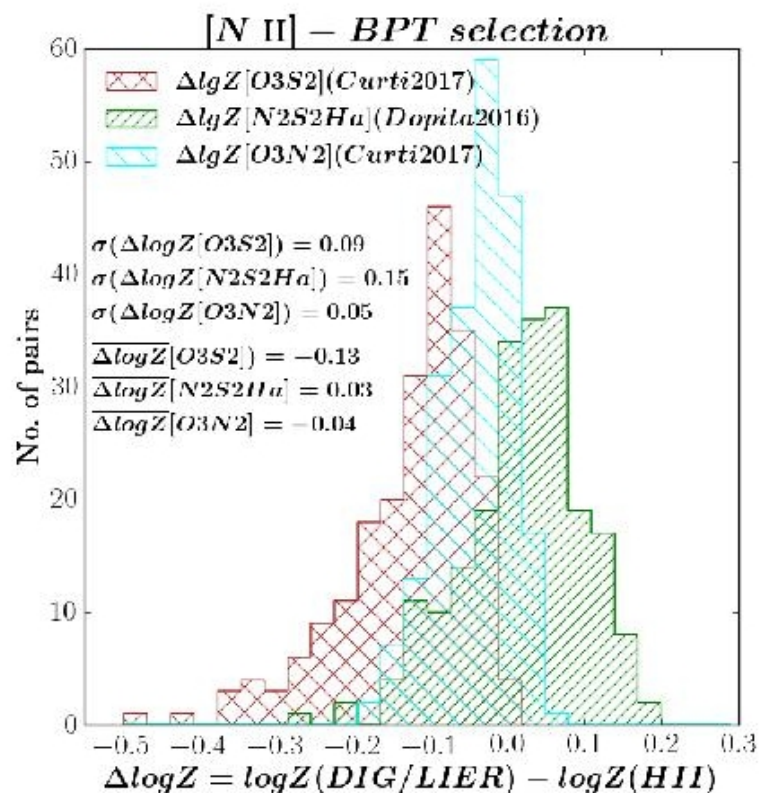
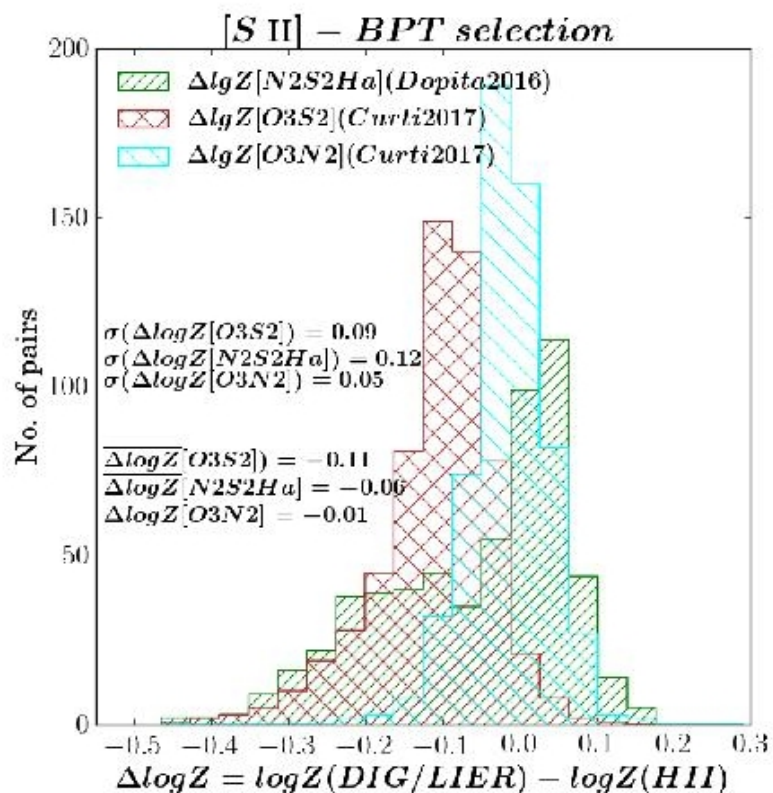
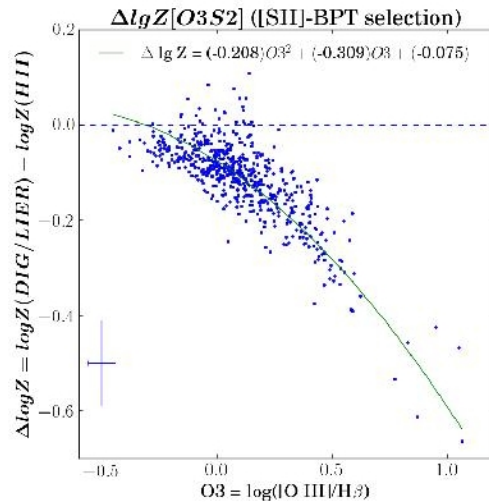
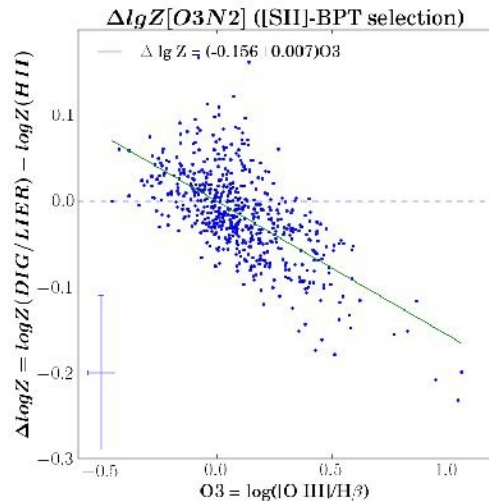
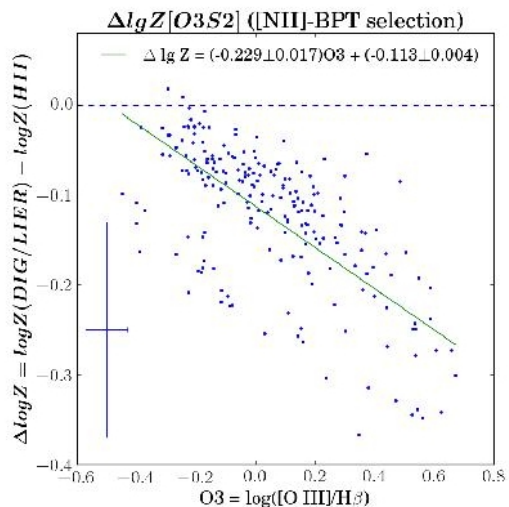
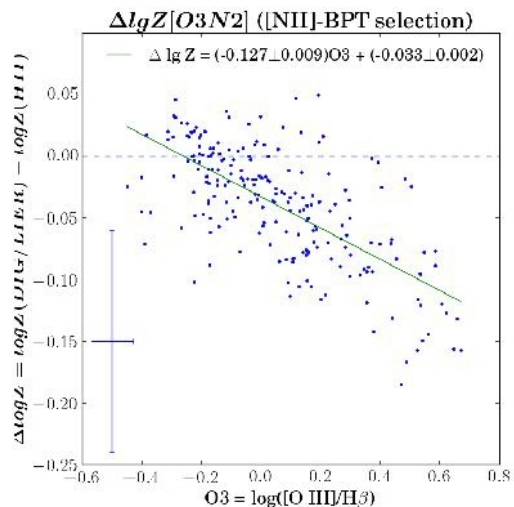


**Figure 1.** Emission line ratio diagnostic [S II]-BPT diagrams (upper panel) and spatially-resolved [S II]-BPT maps (lower panel) of NGC 1042 (left panel), ESO 499-G37 (middle panel) and PGC 3853 (right panel). In all panels, blue, pink and yellow data points denote the data points with emission line ratios corresponding to H II, LIER/DIG and Seyfert, respectively. In the upper panel, each point corresponds to line-ratios in a Voronoi bin, the black solid curve represents the theoretical maximum starburst line from Kewley et al. (2001), providing a demarcation between the bins with H II regions and DIG/LIER-dominated regions. In the DIG/LIER-dominated regime on the BPT diagnostic diagram, the dashed line shows the demarcation between the DIG/LIER and Seyfert regions. The median

# Систематическая ошибка металличности у LIERs



# Корреляция этой ошибки с параметром возбуждения





# Внесли эту поправку...

$$12 + \log(\text{O}/\text{H})_{\text{DIG/LIER}} = x_{\text{O3N2}} + 8.69 + 0.156 \text{ O3} \quad (10)$$

$$12 + \log(\text{O}/\text{H})_{\text{DIG/LIER}} = x_{\text{O3S2}} + 8.765 + 0.309 \text{ O3} + 0.208 \text{ O3}^2$$

$$12 + \log(\text{O}/\text{H})_{\text{DIG/LIER}} = x_{\text{O3N2}} + 8.723 + 0.127 \text{ O3} \quad (14)$$

$$12 + \log(\text{O}/\text{H})_{\text{DIG/LIER}} = x_{\text{O3S2}} + 8.803 + 0.229 \text{ O3} \quad (15)$$

# ...стало хорошо

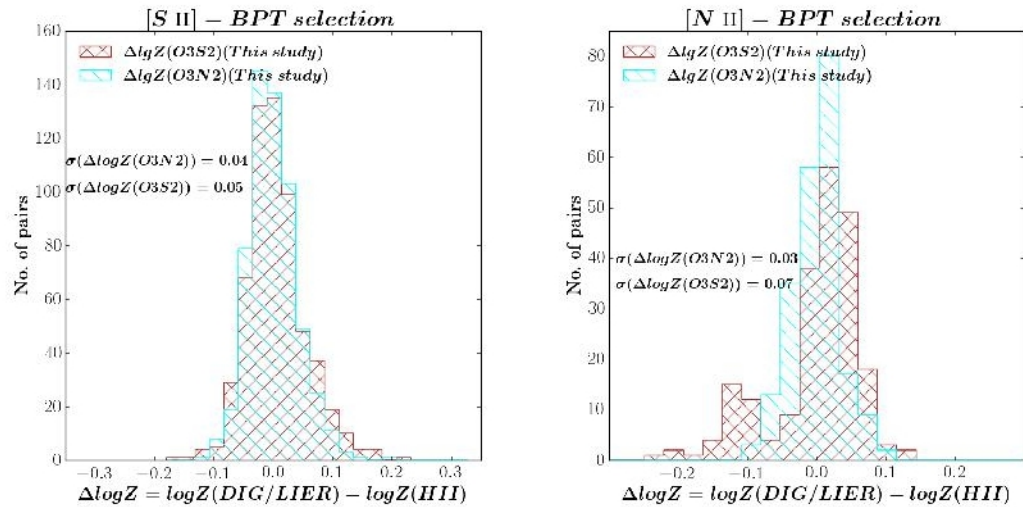


**Figure 9.** Distribution of corrected differential metallicity ( $\Delta \log Z$ ) of H II–DIG/LIER pairs selected on the basis of the [S II]-BPT (left panel) and [N II]-BPT (right panel) diagrams. In each panel brown and cyan histograms represent the differential metallicity distribution from O3S2, and O3N2, respectively after applying the correction to the DIG/LIER/Seyfert spaxels presented in section 4.2 (equations 10, 11, 14, 15).  $\sigma(\Delta \log(Z))$  denotes the standard deviation of the differential metallicity distribution. In each case the average offsets of the distribution are zero by construction.

# ArXiv: 1902.01427

## New constraints on red-spiral galaxies from their kinematics in clusters of galaxies

Akinari Hamabata,<sup>1\*</sup> Taira Oogi,<sup>2</sup> Masamune Oguri,<sup>1,2,3</sup>

Takahiro Nishimichi<sup>4</sup> and Masahiro Nagashima<sup>5</sup>

<sup>1</sup>*Department of Physics, The University of Tokyo, 7-3-1 Hongo, Bunkyo-ku, Tokyo 113-0033, Japan*

<sup>2</sup>*Kavli Institute for the Physics and Mathematics of the Universe, University of Tokyo, Kashiwa, Chiba 277-8583, Japan*

<sup>3</sup>*Research Center for the Early Universe, The University of Tokyo, 7-3-1 Hongo, Bunkyo-ku, Tokyo 113-0033, Japan*

<sup>4</sup>*Center for Gravitational Physics, Yukawa Institute for Theoretical Physics, Kyoto University, Kyoto 606-8502, Japan*

<sup>5</sup>*Faculty of Education, Bunkyo University, 3337 Minami-Ogishima, Koshigaya-shi, Saitama 343-8511, Japan*

Accepted XXX. Received YYY; in original form ZZZ

### ABSTRACT

The distributions of the pairwise line-of-sight velocity between galaxies and their host clusters are segregated according to the galaxy's colour and morphology. We investigate the velocity distribution of red-spiral galaxies, which represents a rare population within galaxy clusters. We find that the probability distribution function of the pairwise line-of-sight velocity  $v_{\text{los}}$  between red-spiral galaxies and galaxy clusters has a dip at  $v_{\text{los}} = 0$ , which is a very odd feature, at 93% confidence level. To understand its origin, we construct a model of the phase space distribution of galaxies surrounding galaxy clusters in three-dimensional space by using cosmological  $N$ -body simulations. We adopt a two component model that consists of the infall component, which corresponds to galaxies that are now falling into galaxy clusters, and the splash-



# Выборка красных галактик

To determine the kinematics of cluster galaxies, we require precise spectroscopic redshifts. For this purpose, we employ the spectroscopic galaxy sample from SDSS DR10 data (Ahn et al. 2014). We use galaxies observed by Legacy spectroscopic observation (York et al. 2000) only, because we have to use galaxies selected by uniform criteria. Following Masters et al. (2010), we select red galaxies based on their `cModelMag`, as  $(g - r) > 0.63 - 0.02(M_r + 20)$ , where  $M_r$  is the absolute magnitude in  $r$  band. We also limit the galaxy sample for our analysis to  $M_r < -20.17$ . For each galaxy, the absolute magnitude is computed from its apparent `cModelMag` with the  $k$ -correction using the technique defined in Chilingarian & Zolotukhin (2012), and also with the correction of Galactic extinction (Schlegel et al. 1998).

Galaxy Zoo is an online citizen science project to obtain morphological information for a large number of galaxies from visual inspections. We use the Galaxy Zoo 1 data release (Lintott et al. 2008), which is the largest morphologically classified sample of galaxies. We select spiral galaxies as  $p_{\text{cs\_debiased}} > 0.8$ , where  $p_{\text{cs\_debiased}}$  is the debiased fraction of votes for combined spiral galaxies with the correction of

# Выборка и распределение по $v$

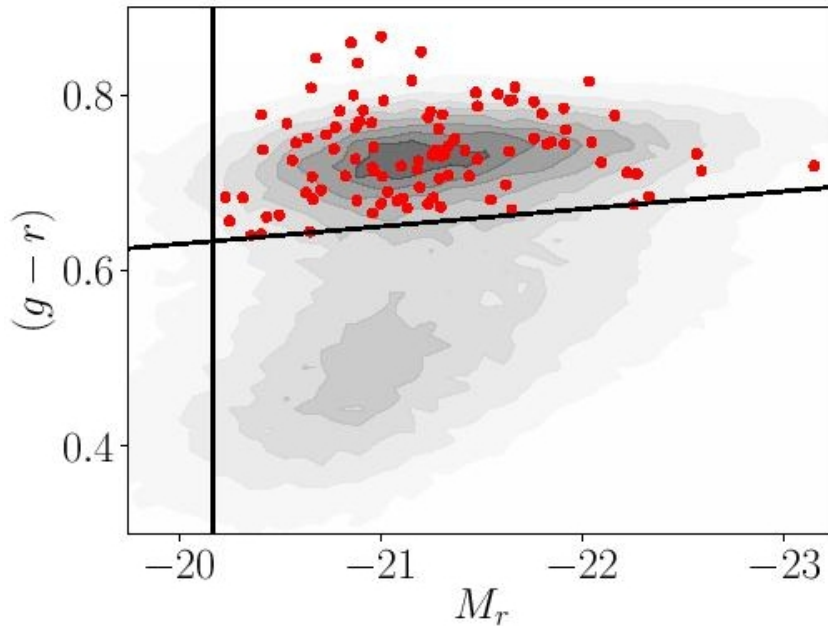


**Figure 1.** Colour-magnitude diagram of our galaxy sample. Red points indicate red-spiral galaxies at  $|z_g - z_c| < 0.01$  within the transverse distance of  $0.5 h^{-1} \text{Mpc}$  from the centre of galaxy clusters at  $0.05 < z < 0.1$  that we use in this analysis. The contours show the number distribution of the Galaxy Zoo 1 sample in the redshift range  $0.05 < z < 0.1$ . The solid lines indicate the colour cut and the absolute magnitude cut adopted in this paper.

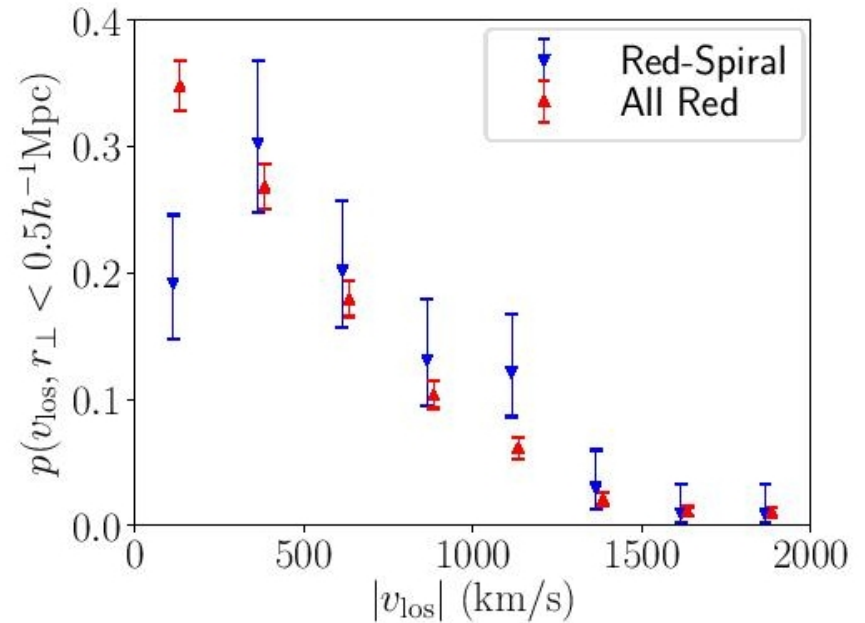


**Figure 2.** The PDF of  $|v_{\text{los}}|$  of red-spiral galaxies (blue triangle down) and red galaxies (red triangle up). Galaxies within projected  $0.5 h^{-1} \text{Mpc}$  from the centre of the clusters are used.

In Fig. 2, we show the PDF of the line-of-sight velocity,  $p(|v_{\text{los}}|)$ , for red-spiral galaxies. For comparison, we also show

# Модель фазового пространства

We use haloes with masses  $M_{200m} > 1 \times 10^{11} h^{-1} M_{\odot}$  to represent galaxy haloes in this work, where  $M_{200m}$  is the mass within  $r_{200m}$ , which is the radius within which the average density is 200 times the background matter density at the redshift of interest. We use haloes with masses  $9.5 \times 10^{13} h^{-1} M_{\odot} < M_{200m} < 2.3 \times 10^{14} h^{-1} M_{\odot}$  to represent cluster haloes, which corresponds to galaxy clusters with  $20 < \lambda < 40$  given the mass-richness relation shown in (Simet et al. 2018, see also Murata et al. 2018), where  $\lambda$  is the richness of galaxy clusters calculated in the redMaPPer. To mimic the observed cluster catalogue, we remove cluster haloes from our analysis if there are any other cluster haloes with larger masses within physical  $1 h^{-1} \text{Mpc}$  from those cluster haloes. We use only snapshots at  $z = 0.1$  in this work.

# Сравнение данных с моделью

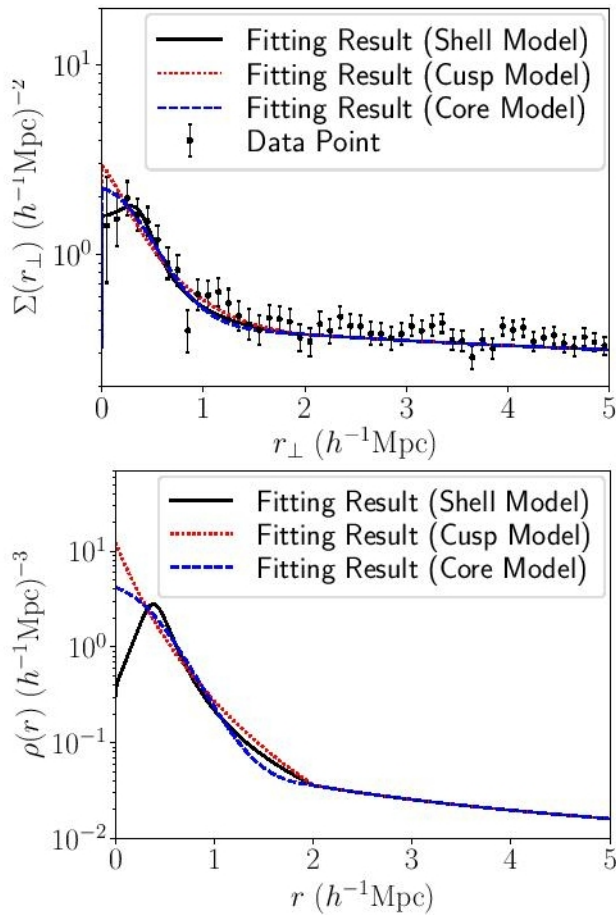


Figure 5. Top : The projected surface density ( $\Sigma(r_{\perp})$ ) of red-spi

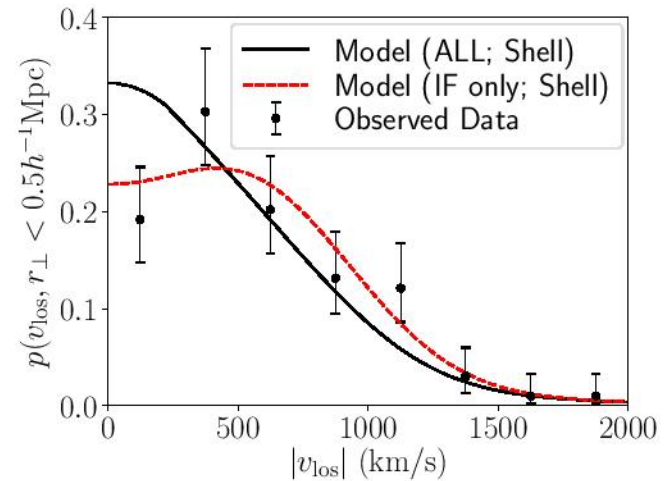
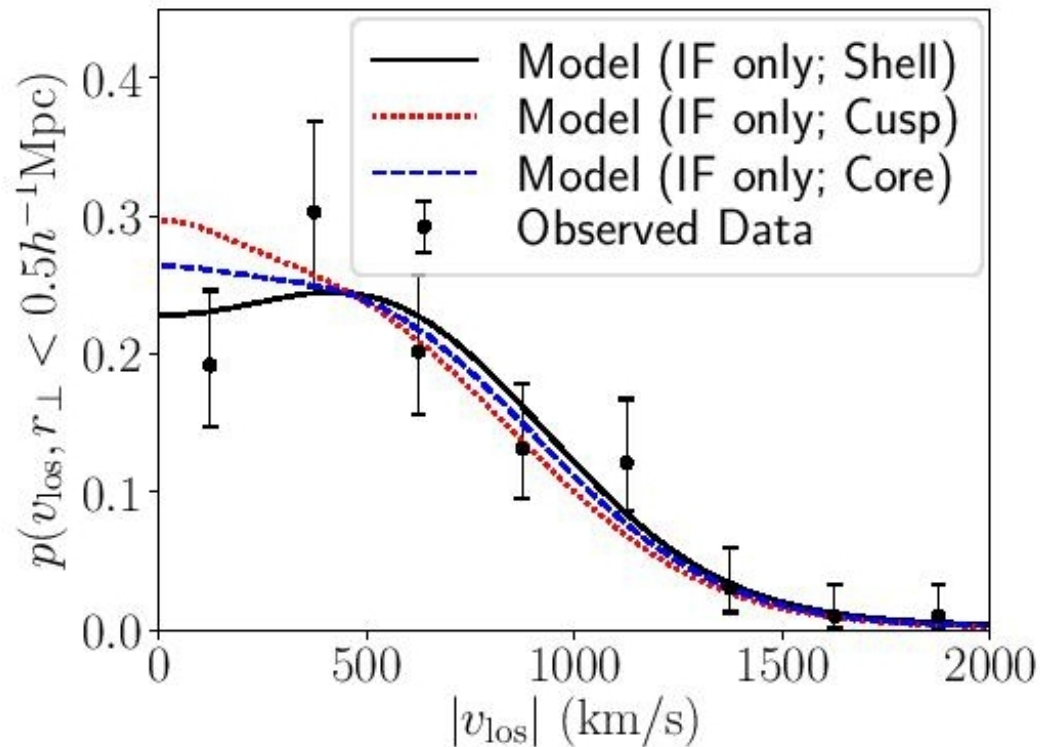


Figure 6. The PDF of  $|v_{\text{los}}|$  of red-spiral galaxies. Points with error bars are the PDF obtained from the observation, the black solid line is the PDF calculated from equation (2), and the red dashed line is the PDF from the infall component only i.e., PDF calculated from equation (2) with  $\alpha(r) = 0$ . We adopt the shell model as the radial distributions of red-spiral galaxies here. The projected aperture adopted here is  $0.5h^{-1}\text{Mpc}$ .

# Интерпретация странноватая...



**Figure 8.** Same as Fig. 7, but with only the infall component, i.e.,  $\alpha = 0$ .